ORIGINAL ARTICLE

WILEY **Cancer Science**

Platforms of in vivo genome editing with inducible *Cas9* for advanced cancer modeling

Norihide Jo[1] | Yuko Sogabe[1] | Yosuke Yamada[1] | Tomoyo Ukai[1,2] |
Harunobu Kagawa[1] | Kanae Mitsunaga[1] | Knut Woltjen[1,3] | Yasuhiro Yamada[1,2,4] (iD)

[1]Department of Life Science Frontiers, Center for iPS Cell Research and Application (CiRA), Kyoto University, Kyoto, Japan

[2]Division of Stem Cell Pathology, Center for Experimental Medicine and Systems Biology, Institute of Medical Science, University of Tokyo, Tokyo, Japan

[3]Hakubi Center for Advanced Research, Kyoto University, Kyoto, Japan

[4]AMED-CREST, Tokyo, Japan

Correspondence
Yasuhiro Yamada, Division of Stem Cell Pathology, Center for Experimental Medicine and Systems Biology, Institute of Medical Science, University of Tokyo, Tokyo, Japan.
Email: yasu@ims.u-tokyo.ac.jp

Funding information
Japan Society for the Promotion of Science, Grant/Award Number: JP16H06276; Naito Foundation; Takeda Science Foundation; Japan Agency for Medical Research and Development, Grant/Award Number: JP18cm0106203 and JP18gm1110004

The emergence of clustered regularly interspaced short palindromic repeat (CRISPR)/Cas9 technology has dramatically advanced how we manipulate the genome. Regarding in vivo experiments, *Cas9*-transgenic animals could provide efficient and complex genome editing. However, this potential has not been fully realized partly due to a lack of convenient platforms and limited examples of successful disease modeling. Here, we devised two doxycycline (Dox)-inducible *Cas9* platforms that efficiently enable conditional genome editing at multiple loci in vitro and in vivo. In these platforms, we took advantage of a site-specific multi-segment cloning strategy for rapid and easy integration of multiple single guide (sg)RNAs. We found that a platform containing *rtTA* at the *Rosa26* locus and *TRE-Cas9* together with multiple sgRNAs at the *Col1a1* locus showed higher efficiency of inducible insertions and deletions (indels) with minimal leaky editing. Using this platform, we succeeded to model Wilms' tumor and the progression of intestinal adenomas with multiple mutations including an activating mutation with a large genomic deletion. Collectively, the established platform should make complicated disease modeling in the mouse easily attainable, extending the range of in vivo experiments in various biological fields including cancer research.

KEYWORDS
complex cancer modeling, CRISPR/Cas9, doxycycline-inducible, in vivo, large genomic deletion

1 | INTRODUCTION

Clustered regularly interspaced short palindromic repeat (CRISPR)/Cas9 has become a common-place genome editing tool as a result of its efficiency, specificity and convenience,[1] and its application in vivo has been extensively explored.[2] Indeed, constitutive mutant rodents have been successfully generated from zygote or ESC transduced with sgRNA and Cas9,[3] and are widely used in a variety of experiments. However, few technological advances have been made for conditional in vivo genome editing with CRISPR/Cas9. One approach is to externally deliver CRISPR/Cas9 directly into the animal's body by various methods such as virus[4] and electroporation;[5] however, low mutation efficiency in the target organ and variation in the resultant mutants may preclude the use of this system for in vivo experiments.

Another approach is *Cas9*-transgenic animals, in which either Cre/loxP-conditional[6,7] or Dox-inducible *Cas9*[8] are used to alleviate the challenges of delivery. Especially in the latter report, sgRNAs were targeted into the genome together with an inducible *Cas9* so that the mice were germline-competent with improved mutation efficiency and homogeneity. Nonetheless, the previous inducible *Cas9*-based platform[8] is suboptimal as a result of the sgRNA loading method, which requires a restriction enzyme-based, one-by-one cloning procedure. In addition, leaky genome editing in vivo has not been fully characterized. Furthermore, modeling cancer with *Cas9*-transgenic animals has been mainly demonstrated by combined loss-of-function mutations, which do not fully reflect the genetic diversity found in human cancers.

To make genome editing with *Cas9*-transgenic animals further accessible, we devised new platforms for efficient genome editing at multiple loci in a Dox-inducible method in vivo. Loading up to four sgRNAs simultaneously into the targeting vector was feasible by using a site-specific multi-segment cloning strategy.[9] A RMCE-[10,11] based platform showed efficient genome editing upon Dox administration while displaying minimal levels of unintended insertions and deletions (indels) in the absence of Dox both in vitro and in vivo. Finally, we used this platform to model cancers with complex genome editing including both activating and inactivating mutations in an inducible way. We propose that these platforms can achieve complex genome editing rapidly and efficiently in vivo.

2 | MATERIALS AND METHODS

2.1 | Construction of targeting vectors

A prototype of Dox-inducible *Cas9* Flp-in vector containing the *IRES-mCherry* cassette for KH2 ESC was described previously.[12] The *Rosa26-tetOP*-("Gateway att" site)-*IRES-mCherry* targeting vector was described previously.[13] *Cas9* ORF was cloned from pX330 plasmid (#42230; Addgene, Watertown, MA, USA). To reduce background expression of Cas9, *tetOP* was replaced with tetracycline response element, third generation (TRE3G, from pTRE3G; Clontech, Mountain View, CA, USA). MultiSite Gateway Cloning Site (MGCS)[9] was cloned upstream of TRE3G by In-Fusion cloning (Clontech).

2.2 | Single guide RNAs and *rtTA3* cloning by MultiSite Gateway technology

The entire cloning process is represented in Results section and Figure 1C. Manufacturer's instructions (Invitrogen, Carlsbad, CA, USA), original paper of MultiSite Gateway technology[9] and the previously

reported multiple lentiviral expression (MuLE) system[14] were used as references to recombine multiple sgRNAs and *rtTA3* into Dox-inducible *Cas9* platforms. Gateway technology enables efficient transfer of DNA fragments between different cloning vectors by BP and LR recombination reactions which use "Gateway att" sites applied from bacteriophage (Invitrogen). Colonies after transformation of the BP and LR reactants were screened by PCR, and a fraction of them were confirmed by Sanger sequencing. PCR cloning was done with KAPA HiFi HotStart ReadyMixPCR Kit (KAPA Biosystems, Wilmington, MA, USA).

2.3 | Establishment of Dox-inducible *Cas9* ESC

The RMCE-based targeting vector (RC platform) with the desired sgRNAs was electroporated into KH2 ESC using a previously described method.[10] Hygromycin-resistant colonies were selected, expanded and confirmed to be sensitive for G418 Disulfate Aqueous Solution (G418) (Nacalai Tesque, Kyoto, Japan). Homologous recombination-based *Rosa26* targeting vector (R-platform) with the desired sgRNAs (10-20 μg) was electroporated into V6.5 ESC. Blasticidin-resistant colonies were selected and expanded. The clones were screened by PCR genotyping and confirmed to be positive for mCherry signal with Dox treatment.

### 2.4 | In vitro culture of ESC and mouse embryonic fibroblasts

Cells were maintained at 37°C with 5% CO_2. ESC were maintained with feeders in ESC culture medium (knockout DMEM containing 2 mmol/L L-glutamine, 1× nonessential amino acids (NEAA) (Nacalai Tesque), 100 U/mL penicillin, 100 μg/mL streptomycin (P/S) (Nacalai Tesque), 15% FBS (Gibco, Gaithersburg, MD, USA), 0.11 mmol/L β-mercaptoethanol (Gibco) and 1000 U/mL human recombinant leukemia inhibitory factor (LIF) (Wako, Osaka, Japan) or without feeders in alternative 2i (a2i) culture medium, which was supplemented with 1.5 μmol/L CGP77675 (Sigma, St Louis, MO, USA) and 3 μmol/L CHIR99021.[15,16] Mouse embryonic fibroblasts (MEF) were isolated from E15.5 embryos and cultured in DMEM (Nacalai Tesque) with 2 mmol/L L-glutamine, 1× NEAA, P/S, 10% FBS and 0.11 mmol/L β-mercaptoethanol. Immunofluorescence signals were detected by BZ-9000 (Keyence, Osaka, Japan).

### 2.5 | Green fluorescent protein labeling of ESC

KH2 ESC with three sgRNAs targeting *EGFP*, *Cdh1* and *Lmna* and V6.5 ESC were labeled by *Rosa26*-targeting vector carrying

FIGURE 1 Platforms for doxycycline (Dox)-inducible genome editing at multiple loci. A, Overview of the RC and R platforms with three single guide (sg)RNAs targeting the *Col1a1* locus of KH2 ES cells or the *Rosa26* locus of parental V6.5 embryonic stem cells (ESC), respectively. mCh, mCherry; IRES, internal ribosome entry site; PGK, phosphoglycerate kinase; rtTA, reverse tetracycline transactivator; TRE3G, tetracycline response element, 3rd generation. B, Schematic representation of targeting vectors containing MultiSite Gateway Cloning Site (MGCS) for loading sgRNAs. Blast, blasticidin-resistance gene; HA, homology arm; SApA, splice acceptor and poly A. C, Representative vector construction process from three template plasmids (eg, pX330) to destination vectors of the RC and R platforms. In the case of the R platform, PGK-*rtTA3*-pA sequence was additionally recombined to induce *Cas9* from a single *Rosa26* allele. D, Efficiency of the BP (left) and LR (right) reactions. Efficiency was calculated based on the results of PCR, which were highly consistent with those of Sanger sequencing (data not shown). Numbers in parentheses indicate the number of reactions carried out in this study. NA, not available
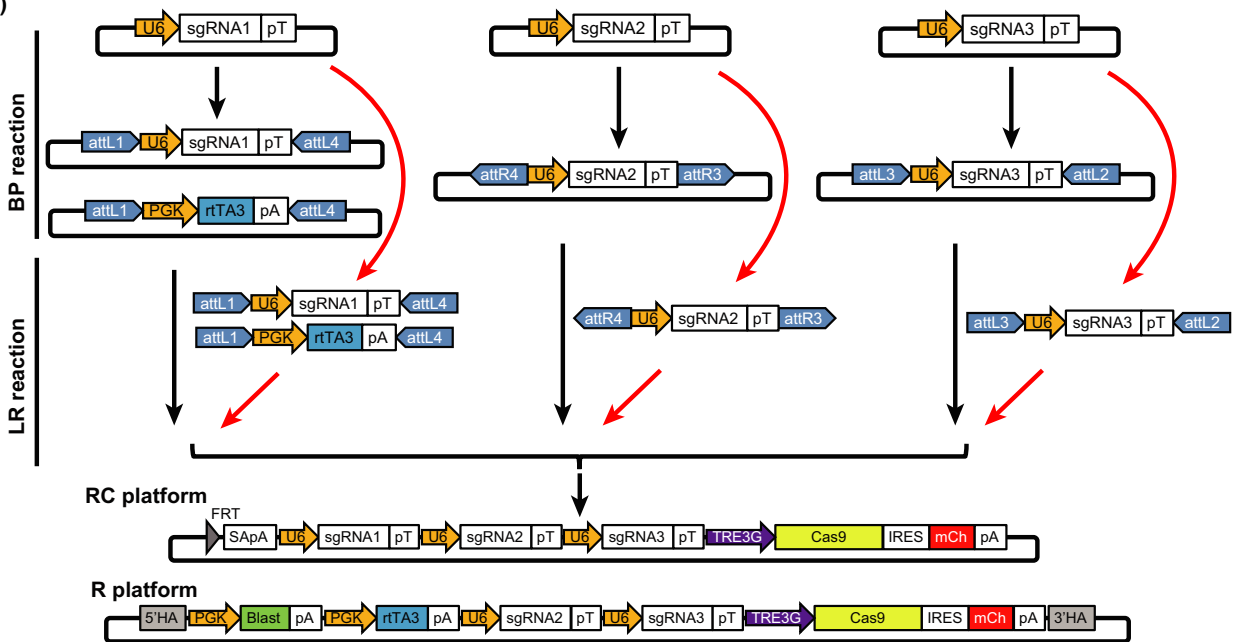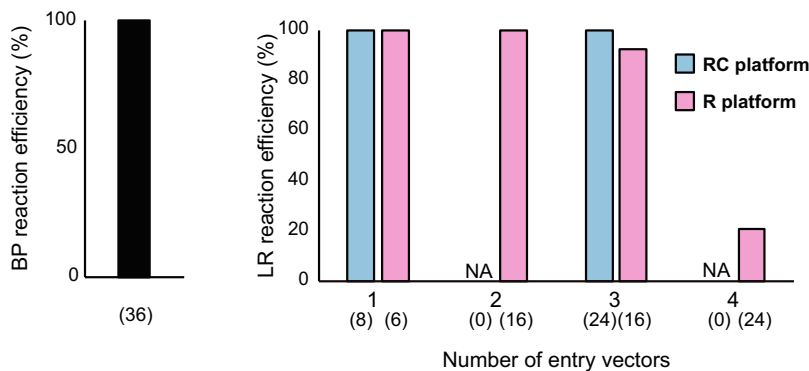
(A) RC platform

(B)
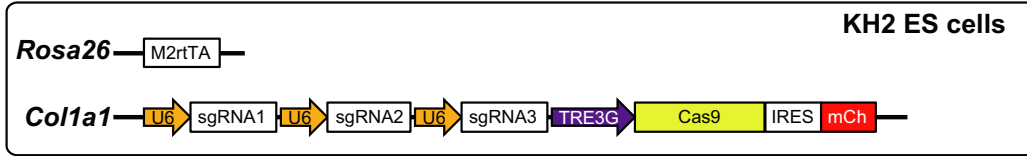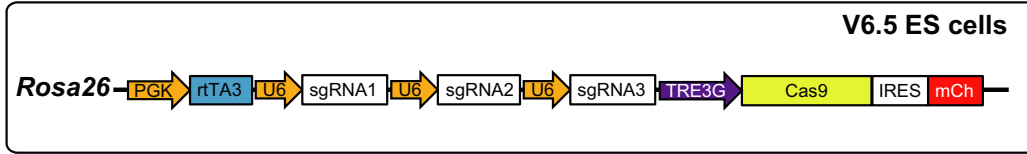
(C)

(D)

CAG-loxP-PGK-Neo-3xpA-loxP-EGFP. Briefly, 20 µg of the targeting vectors was electroporated into the ESC, and G418 (350 µg/mL)-resistant colonies were selected and expanded. Subsequently, the Cre-expressing plasmid was electroporated into the selected ESC to recombine loxP and to express EGFP. EGFP-positive colonies were selected and screened by PCR. KH2 ESC with *EGFP* sgRNA alone were labeled by *piggyBac* (PB) transposon carrying *CAG-EGFP-IRES-Neo.*[17] Transposon plasmid (2.5 µg) and transposase expression vector (2.5 µg) were transfected into ESC using Xfect mESC Transfection Reagent (Clontech) according to the supplier's protocol. Transfected cells were selected by G418. EGFP-positive colonies were selected and established as EGFP-labeled clones.

2.6 | Animals

All animal studies were conducted in compliance with the ethical regulations of Kyoto University and University of Tokyo, and were approved by the Center for iPS Cell Research and Application (CiRA), Kyoto University, and the Institute of Medical Science, the University of Tokyo. All mice were maintained in a specific pathogen-free facility. C57BL/6, ICR and pseudopregnant ICR mice were purchased from Japan SLC. Midday on the day when the plug was observed was designated as embryonic day (E) 0.5.

2.7 | Chimera formation

Female ICR mice were treated with pregnant mare serum gonadotropin (PMSG; 7.5 IU) and human chorionic gonadotropin (hCG; 7.5 IU) by i.p. injection. Embryos were rinsed with M2 medium (Sigma) and cultured in KSOM medium until development into blastocysts. ESC were tested for *Mycoplasma* contamination before blastocyst injection. Two to seven cells per embryo were injected into the blastocoels of E3.5 blastocysts. Injected blastocysts were transferred into the uteri of pseudopregnant ICR mice.

2.8 | Doxycycline treatment

For cultured cells, Dox was used at a concentration of 2.0 µg/mL. For in vivo modeling, 2.0 mg/mL Dox was continuously given in drinking water supplemented with 10 mg/mL sucrose for the period indicated in each figure. In the case of targeting *EGFP, Cdh1* and *Lmna* in vivo, an additional i.p. injection of Dox was carried out to induce rapid and uniform transgene expression (1.0 mg/injection every 12 hours until analysis).

2.9 | Hematoxylin-eosin staining, immunohistochemistry and immunofluorescence

Samples were fixed with 4% paraformaldehyde overnight at 4°C and embedded in paraffin using Spin Tissue Processor STP120-2 (Thermo Fisher Scientific, Waltham, MA, USA). Sections were stained with H&E. Sections were treated with xylene and 100%

ethanol and then washed with water followed by treatment with Histofine (Nichirei Biosciences, Tokyo, Japan). After rinsing with PBS, sections were incubated with the following antibodies: anti-β-catenin (610153, dilution 1:300; BD Transduction Laboratories, San Jose, CA, USA), anti-Ki67 (ab16667, 1:200; Abcam, Cambridge, UK), anti-PCNA (sc-56, 1:100; Santa Cruz Biotechnology, Dallas, TX, USA), anti-Six2 (11562-2AP, 1:600; Proteintech, Rosemont, IL, USA), anti-GFP (for immunohistochemistry, ab183734, 1:200; Abcam, for immunofluorescence, 4B10, 1:100; CST, Danvers, MA, USA) and anti-mCherry (ab167453, 1:600; Abcam). For immunohistochemistry, sections were rinsed with PBS and incubated with Histofine Simple Stain MAX PO (Nichirei) containing secondary antibody for 25 minutes at room temperature. DAB Substrate Kit (Nichirei) was used for detection. For immunofluorescence, the sections were rinsed with PBS and incubated with secondary antibodies conjugated with Alexa 488 (A11029; Invitrogen), 594 (A11037, dilution 1:200; Invitrogen) and DAPI (D21490, dilution 1:500; Invitrogen). Immunofluorescence signals were detected by LSM 700 (Carl Zeiss, Oberkochen, Germany). Statistical analysis for mitotic figures was carried out using Prism 7 Software (GraphPad).

2.10 | Flow cytometry

Small intestine and thymus were incubated in 1% collagenase type 1 for 15 minutes at 37°C. Single-cell suspensions were obtained by transfer through nylon mesh to remove large clumps, repeated washing and centrifugation. Small intestine was additionally incubated with 0.25% trypsin/1 mmol/L EDTA for 15 minutes at 37°C. Cells were analyzed and sorted by FACS (Aria II; BD Biosciences, San Jose, CA, USA).

2.11 | Genomic DNA extraction, cDNA cloning, Sanger sequencing and TIDE analysis

For DNA extraction, ESC, MEF or cells sorted by flow cytometry were directly lysed in DNA lysis buffer (100 mmol/L Tris HCl pH 8.0, 0.2% SDS, 5 mmol/L EDTA, 200 mmol/L NaCl, 1% Proteinase K), followed by precipitation with isopropanol and dissolved in TE buffer. Genomic DNA from the other tissue samples in vivo was extracted by PureLink Genomic DNA Mini Kit (Invitrogen). PCR was carried out with GoTaq Green Master Mix (Promega, Madison, WI, USA). PCR products were purified by FastGene Gel/PCR Extraction Kit (NIPPON Genetics, Tokyo, Japan) and cloned into pCR4-TOPO vector (Invitrogen). The reactants were transformed into DH5α competent *Escherichia coli*, and the grown colonies were analyzed by Sanger sequencing with M13 Reverse primer and with ABI 3500xL (Applied Biosystems, Foster City, CA, USA). TIDE software was used to determine the spectrum and frequency of targeted mutations generated in a pool of cells by genome editing tools such as CRISPR/Cas9.[18] TIDE software parameters used in this study were as follows: left boundary, 100 bp; right boundary, −10 bp; decomposition window, 115-685 bp; indel size range, 20 bp.

2.12 | Quantitative RT-PCR

Quantitative PCR was carried out using GoTaq qPCR Mater Mix and CXR Reference Dye according to the supplier's instruction (Promega). StepOnePlus Real-Time PCR system (Applied Biosystems) was used. Transcript levels were normalized by β-actin. Experiments were carried out in triplicate. Primers used are shown in Table S1.

3 | RESULTS

3.1 | Platforms for Dox-inducible genome editing at multiple loci

We devised two types of targeting vectors for RMCE-based KH2 ESC and the parental ESC (V6.5) to establish the RC platform and the R platform for Dox-inducible genome editing, respectively (Figure 1A,B). KH2 cells are mouse ESC that have an FRT recombination site for Flp-in integration of a single-copy transgene at the *Col1a1* safe harbor locus and express the reverse tetracycline-regulated transactivator (*M2rtTA*) under the endogenous *Rosa26* promoter, enabling Dox-inducible transgene expression.[10] Both the RC and R platform vectors have MGCS to accommodate up to four sgRNAs in tandem in conjunction with a Dox-inducible *Cas9* (Figure 1B). An IRES-*mCherry* sequence was designed downstream of *Cas9* to visualize the induced *Cas9* expression (Figure 1B). The general recombination process is represented in Figure 1C. Briefly, desired sgRNAs were first prepared in template expression plasmids such as pX330.[19] Next, sequences for RNA polymerase III promoter (eg, U6), sgRNA and TTTTTT poly-T (pT) termination were subcloned into pDONR vectors by PCR with specific primers for the BP reaction (Table S1) to generate entry clones. Finally, the prepared entry clones were simultaneously recombined by the LR reaction with the targeting vectors for either the RC platform or the R platform. Alternatively, sequences for the U6 promoter, sgRNA and pT were PCR-amplified from the pX330 template plasmid by long primers that contain the attL or attR site (Table S1), and were directly applied to the LR reaction. Both BP and LR reactions were highly efficient throughout the study, requiring only 5 to 7 days to prepare targeting vectors (Figure 1D). Although RMCE at the *Col1a1* locus was efficient, we detected the unrecombined fragment of the targeting vector in one out of nine RC-ES cell lines (data not shown), suggesting that random integrations infrequently occur in this system.[10]

3.2 | Doxycycline-inducible genome editing at multiple loci in ESC

To verify the utility of our platforms for inducible gene editing, we established ESC with RC platform (RC-ES cells) and R platform (R-ES cells), which contain three sgRNAs that target *EGFP*, *Cdh1* and *Lmna* and are EGFP-labeled (Figure 2A). *Cdh1* and *Lmna* encode E-cadherin, an adhesion protein, and Lamin A, a component of nuclear lamina, respectively. Throughout this study, we used previously reported TIDE software to analyze the indel frequencies and

patterns.[18] Most RC-ES cells lost their EGFP signal within 72 hours after Dox treatment, but maintained high EGFP signals in the absence of Dox treatment (Figure 2B-D). Colonies of RC-ES cells became fragile after Dox treatment (Figure 2B), presumably because of genetic ablation of *Cdh1* and/or *Lmna*. Genomic DNA analysis showed that Dox treatment induced a high frequency of total indels at the *Cdh1* and *Lmna* loci in RC-ES cells, whereas minimal indels were detectable in the absence of Dox treatment, although we did observe variation in the frequency of indels among clones (Figure 2E). The in-frame to out-of-frame indel ratio varied from 1:20 to 1:5, and the preferences of indel patterns were different depending on each sgRNA (Figure S1A).

In contrast, R-ES cells inefficiently lost their EGFP signals in response to Dox treatment (Figure 2B-D). Furthermore, R-ES cell colonies showed a mosaic pattern of EGFP signals and slightly fragile morphology even in the absence of Dox treatment (Figure 2B-D), suggesting leaky genome editing. Consistently, genomic DNA analysis showed that the frequency of indels was lower in Dox-treated R-ES cells compared with Dox-treated RC-ES cells (Figure 2D). Furthermore, indels at the *Cdh1* locus were detectable in up to 20% of alleles even without Dox exposure (Figure 2E). These data indicate that the R platform shows leaky and less efficient genome editing than the RC platform in vitro.

3.3 | Minimal indels without Dox in RC-ES cells

As previously reported, the simultaneous loading of constitutively expressed sgRNAs and an inducible *Cas9* risk unintended mutations before giving Dox.[8] Indeed, the results above showed minimal and some indels in the RC and R platforms, respectively. Given that the Dox-treated ESC colonies often showed fragile morphology, *Cdh1* and/or *Lmna* ablations may have an effect on cell viability, which should affect the calculated efficiency of the genome editing. To investigate indel frequencies in an unbiased way, we next established EGFP-labeled RC-ES cells and R-ES cells, in which *EGFP* sgRNA alone was targeted in either platform (Figure 2F). As expected, RC-ES cells showed minimal indels without Dox even after 10 passages (p10; Figure 2G,H). In contrast, R-ES cells had up to 25% of indels at p3 and p10 in the absence of Dox treatment (Figure S1B and Figure 2H). We also confirmed the efficient induction of genome editing even after four passages in RC-ES cells (Figure 2G,H). These data showed that the RC platform generates minimal indels in the absence of Dox, whereas the R platform displays significant leaky genome editing even without Dox treatment. As the existence of indels at baseline hinders conditional genome editing in vivo, we used the RC platform for all subsequent experiments.

3.4 | Doxycycline-inducible genome editing at multiple loci in somatic cells both in vitro and in vivo

To further examine the applicability of the RC platform in somatic cells, the established RC-ES cells were used directly for
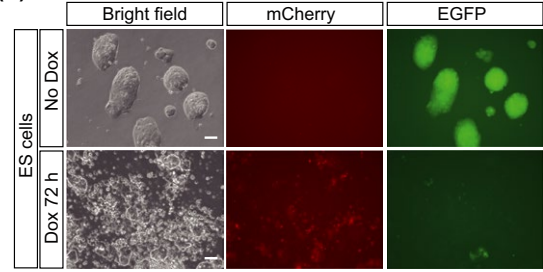
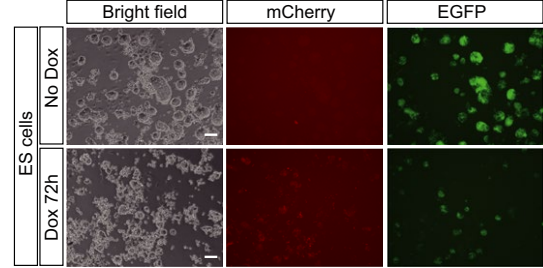**(A)** RC platform (sg*EGFP/Cdh1/Lmna*)

(B) RC-ES cells (sg*EGFP/Cdh1/Lmna*)

R platform (sg*EGFP/Cdh1/Lmna*)
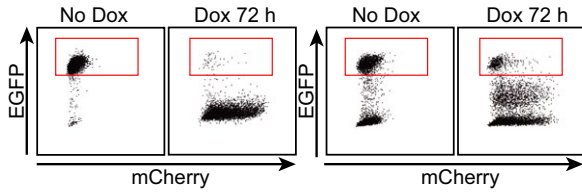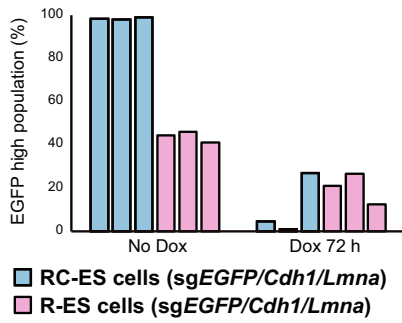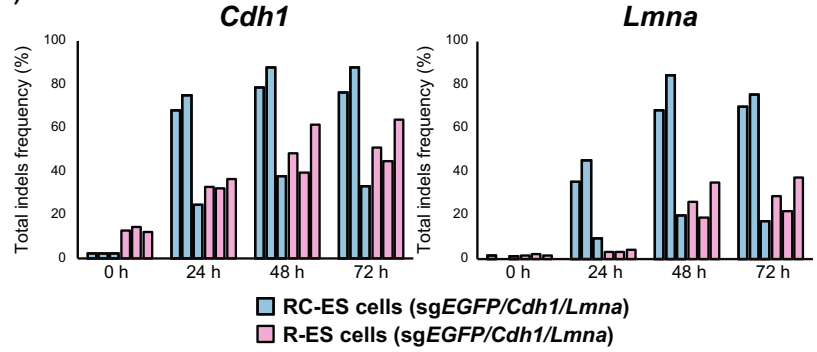
R-ES cells (sg*EGFP/Cdh1/Lmna*)

(C) RC-ES cells (sg*EGFP/Cdh1/Lmna*)   R-ES cells (sg*EGFP/Cdh1/Lmna*)

(D)

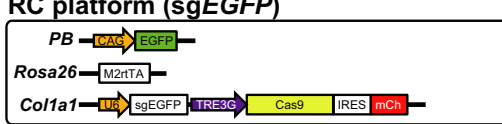RC-ES cells (sg*EGFP/Cdh1/Lmna*)

R-ES cells (sg*EGFP/Cdh1/Lmna*)

(E)

Cdh1   *Lmna*

RC-ES cells (sg*EGFP/Cdh1/Lmna*)

R-ES cells (sg*EGFP/Cdh1/Lmna*)

(F) RC platform (sg*EGFP*)
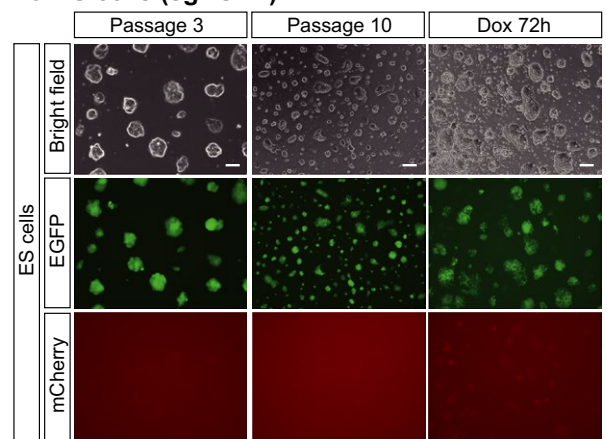
(G) RC-ES cells (sg*EGFP*)

R platform (sg*EGFP*)
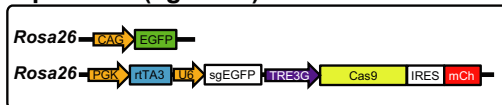
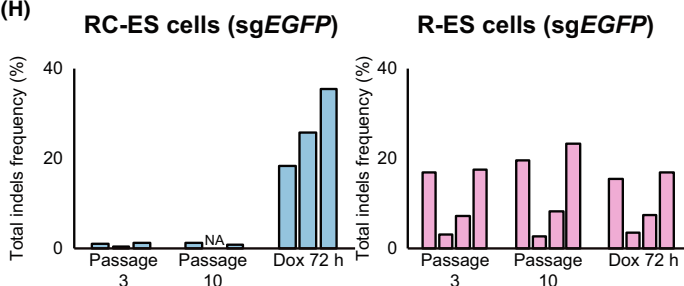**(H)** RC-ES cells (sg*EGFP*)   R-ES cells (sg*EGFP*)

FIGURE 2 Doxycycline (Dox)-inducible genome editing at multiple loci in ES cells. A, Schematic representation of the alleles in the RC and R platforms used in B-E. Both platforms contain an enhanced green fluorescent protein (*EGFP*)-expressing allele together with three single guide (sg)RNAs targeting *EGFP*, *Cdh1* and *Lmna*. B, Bright field and immunofluorescence images of embryonic stem cells (ESC) with the RC and R platforms (RC-ES cells and R-ES cells, respectively). Representative images of three independent ESC clones at p3 are shown. Scale bars, 300 μm. C, Flow cytometric analysis of Dox-treated RC-ES and R-ES cells. Representative dot plots of three independent ES cell clones at passage 3 are shown. D, Ratio of the EGFP high population in (C) (red rectangle). E, Kinetics of insertions and deletions (indel) frequencies at the *Cdh1* and *Lmna* loci. For indel patterns, see also Figure S1A. F, Schematic representation of the alleles in the RC and R platforms used in (G) and (H). RC- and R-ES cells were EGFP-labeled by *piggyBac* (PB) transposition and *Rosa26* targeting, respectively. G, Representative bright field and immunofluorescence images of the RC-ES cells at p3, p10, and ES cells at p4 after Dox exposure for 72 h. Scale bars, 300 μm. See also Figure S1B. H, Total indel frequencies at p3, p10, and ES cells at p4 after Dox exposure for 72 h. Three independent clones for RC-ES cells and four independent clones for R-ES cells were analyzed. NA, not available

blastocyst injection to create chimeric mice. We first established MEF from RC-ES cell-derived chimeric mice (RC-MEF). Consistent with efficient genome editing in RC-ES cells, a high frequency of indels at all three loci was induced in RC-MEF 72 hours after Dox treatment (Figure 3A and Figure S2A). A small extent of indels was also observed in RC-MEF without Dox treatment, suggesting that leaky editing occurs in RC-MEF at low frequencies (Figure 3A).
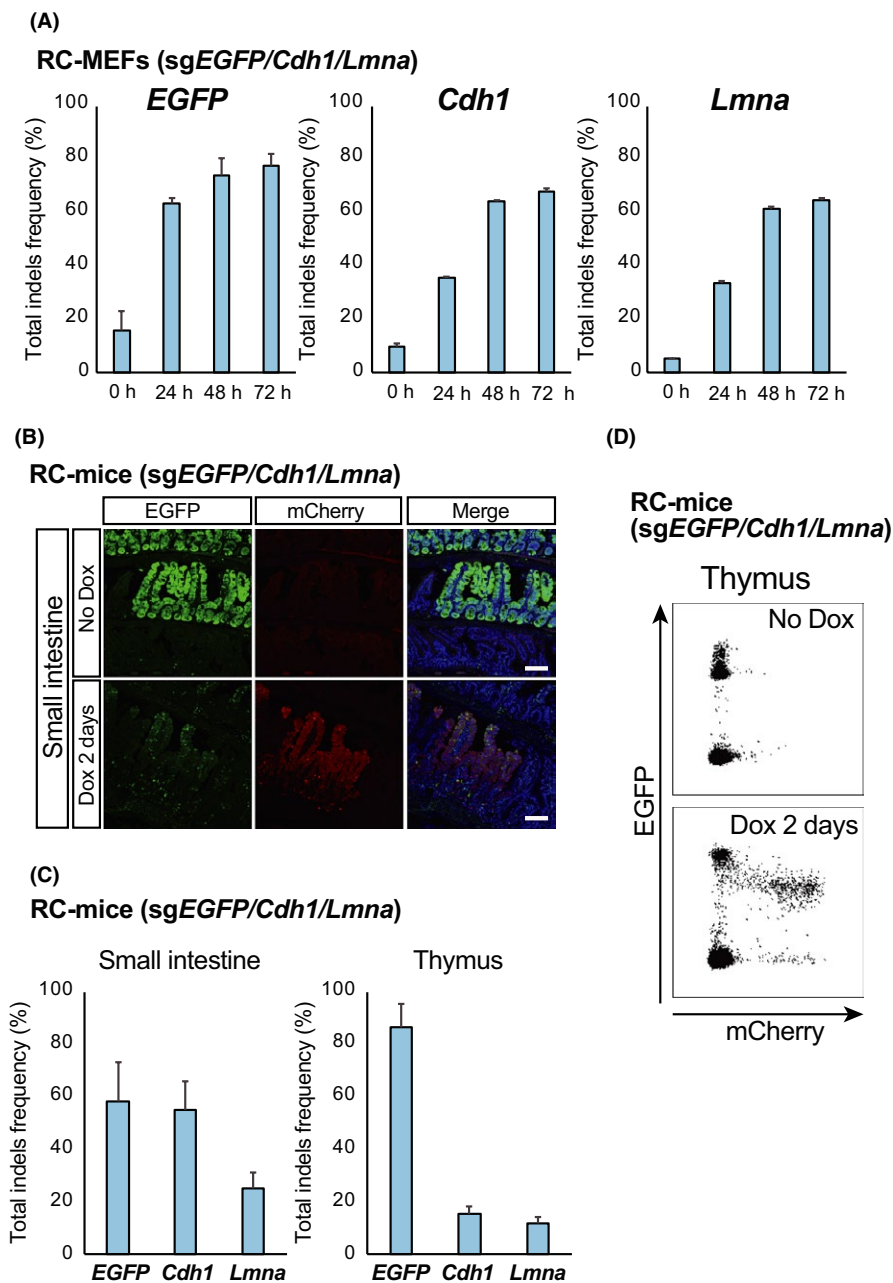
(A)

RC-MEFs (sg*EGFP/Cdh1/Lmna*)

(B)

RC-mice (sg*EGFP/Cdh1/Lmna*)

(C)

RC-mice (sg*EGFP/Cdh1/Lmna*)

(D)

RC-mice (sg*EGFP/Cdh1/Lmna*)

Thymus

FIGURE 3 Doxycycline (Dox)-inducible genome editing at multiple loci in somatic cells both in vitro and in vivo. A, Kinetics of insertions and deletions (indel) frequencies at the enhanced green fluorescent protein (*EGFP*), *Cdh1* and *Lmna* loci of mouse embryonic fibroblasts established from RC-embryonic stem (ES) cell-derived chimeric mice (RC-MEF) treated with Dox (2.0 μg/mL). Data are shown as mean ± SD (n = 3). B, Immunofluorescent staining of the small intestine of RC-chimeric mice containing single guide (sg)RNAs targeting *EGFP*, *Cdh1* and *Lmna*. Scale bars, 100 μm. C, Indel frequency analysis of the small intestine and thymus in RC-chimeric mice containing sgRNAs targeting *EGFP*, *Cdh1* and *Lmna*. Total indel frequencies were analyzed in the mCherry-positive population after 2 days of Dox treatment in 5-week-old mice. Small intestine, n = 2; thymus, n = 3. Data are shown as mean ± SD. D, Representative flow cytometric analysis of the thymus of RC-chimeric mice containing sgRNAs targeting *EGFP*, *Cdh1* and *Lmna*. Three independent thymi were analyzed
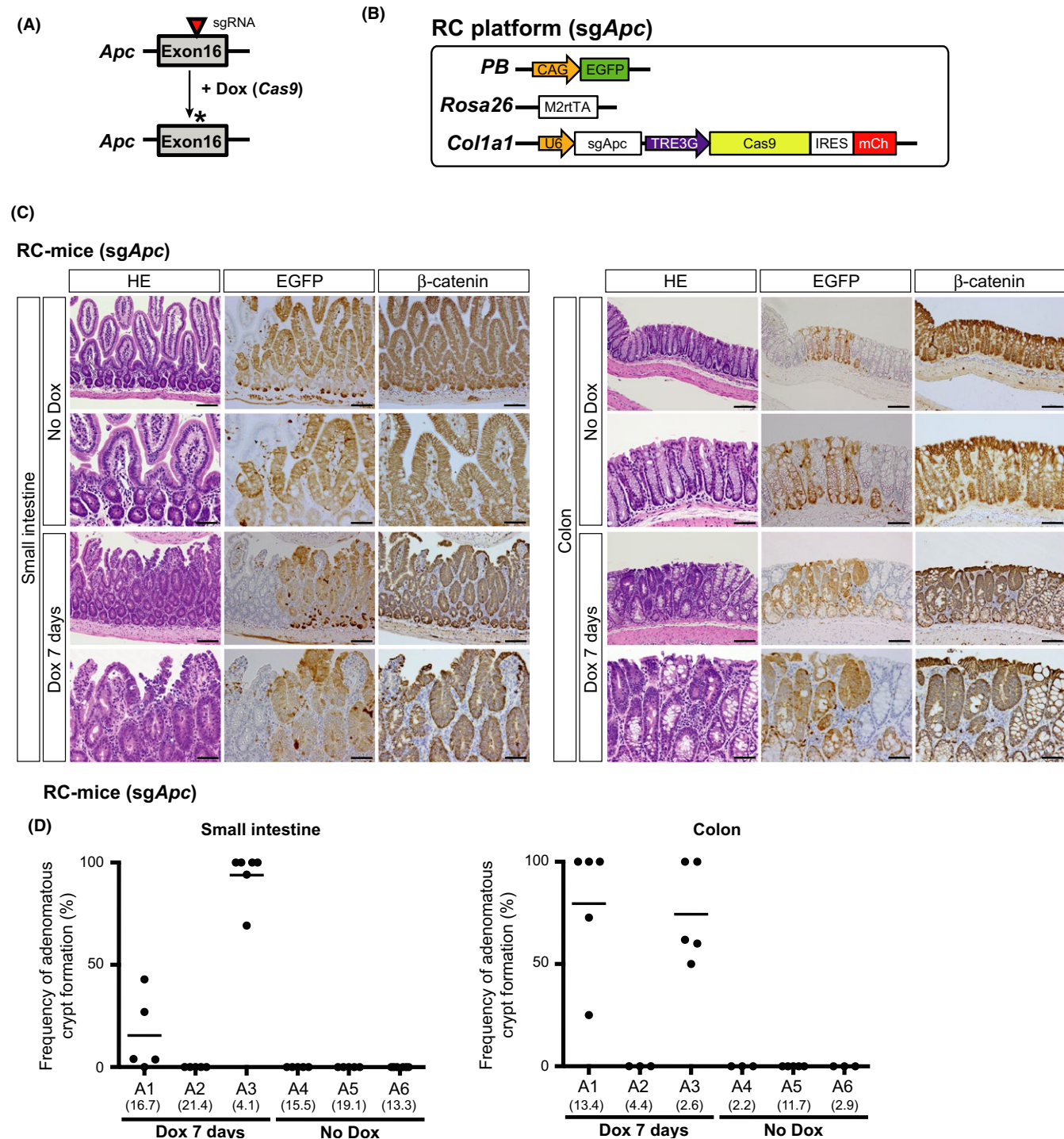
FIGURE 4 Evaluation of impaired *Apc* function after genome editing in adult intestinal cells. A, Design of single guide (sg)RNAs to induce insertions and deletions (indels) at exon 16 of the *Apc* gene. Asterisk indicates indels. B, Schematic representation of the alleles in the RC platform used in this figure. C, RC-chimeric mice were treated with doxycycline (Dox) starting at 5 weeks of age and analyzed at 6 weeks of age. Embryonic stem cell (ESC)-derived intestinal cells are labeled with enhanced green fluorescent protein (EGFP). Scale bars, 100 μm (upper panel) and 50 μm (lower panel). D, Frequency of adenomatous crypt formation in Dox-treated and untreated RC-mice (A1-A6). Frequency of adenomatous crypts was determined in a randomly selected area of EGFP-expressing crypts (n = 3-6/mouse). Number in parentheses indicates the local contribution percentage of ESC-derived cells in each tissue. Data are shown as the scatter plot with the mean

Finally, we treated the RC-ES cell-derived chimeric mice with Dox (RC-mice). mCherry signals were observed in multiple organs of RC-mice after 2 days of Dox treatment, indicating a broad

spectrum of *Cas9* expression throughout the body (Figure 3B and Figure S2B). In the small intestine, the total indel frequencies in the mCherry-positive population reached 80% at the *EGFP* and
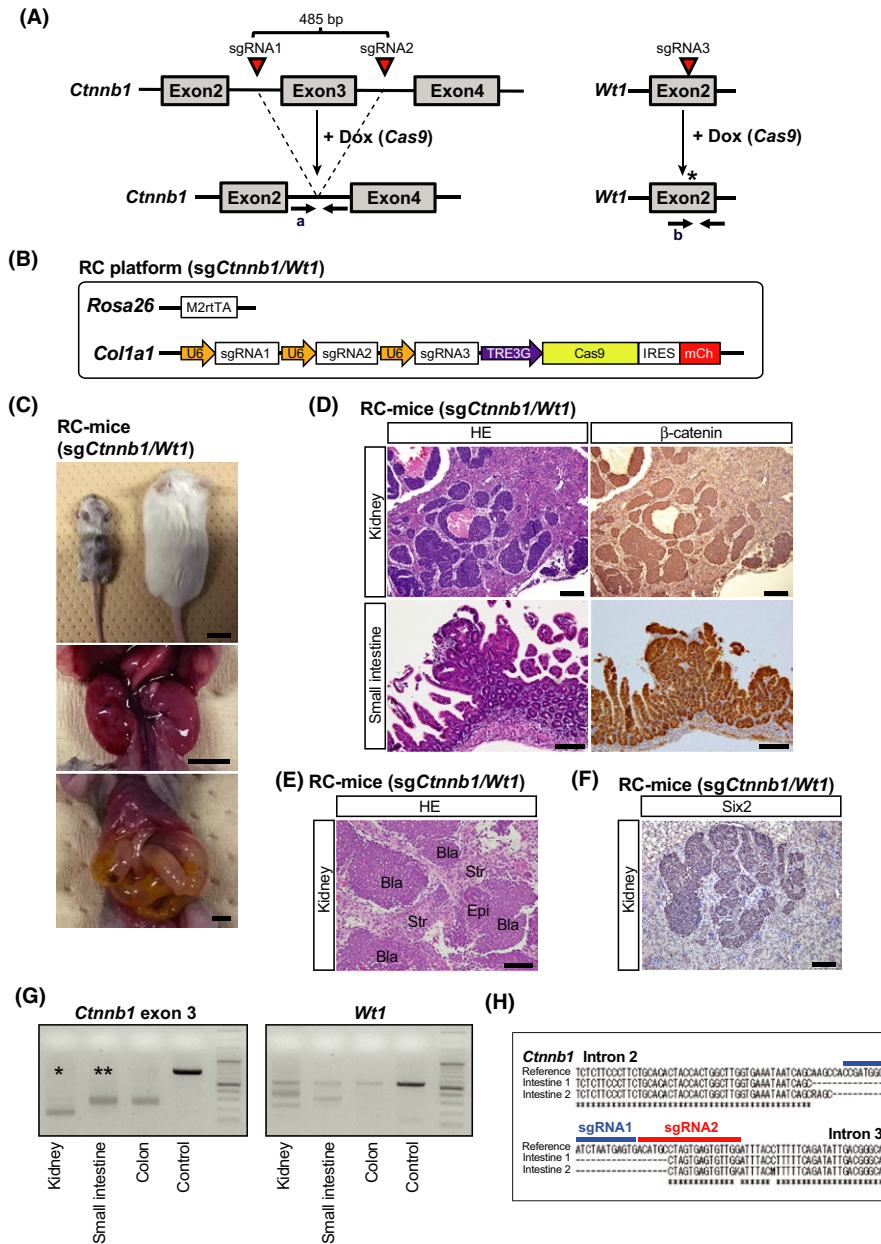
FIGURE 5 Modeling Wilms' tumor with *Ctnnb1* exon 3 deletion and insertions and deletions (indels) at *Wt1* gene. A, Strategy and design of single guide (sg)RNAs (red arrowheads) to induce *Ctnnb1* exon 3 deletion and indels at *Wt1* gene. Asterisk indicates indels. B, Schematic representation of the alleles in the RC platform for Wilms' tumor modeling. C, Upper panel: Chimeric and non-chimeric littermates were treated with doxycycline (Dox) starting at E14.5 and analyzed at 2 weeks of age. Scale bar, 1000 μm. Middle panel: Kidneys show swelling with hemorrhage. Scale bar, 500 μm. Lower panel: Dilated gastrointestinal tract is observed in Dox-treated chimeric mice. Scale bar, 250 μm. D, Histological analysis and β-catenin immunohistochemistry of tumors in the kidney and intestine. Scale bars, 500 μm (kidney) and 100 μm (small intestine). See also Figure S3A. E, Three histological components of Wilms' tumor (blastemal [Bla], stromal [Str] and epithelial [Epi] elements) can be observed in the kidney tumor. Scale bar, 100 μm. F, Six2 immunostaining of the kidney tumor. Scale bar, 100 μm. G, PCR analysis to examine the deletion of *Ctnnb1* exon 3 and indels at the *Wt1* gene. Primers used (a and b) are indicated in (A). Non-chimeric littermates were used as control. H, Sanger sequencing of genomic DNA at *Ctnnb1* exon3 cloned from the PCR product of small intestine (**) in (G). Eight subcloned genomic DNAs per tissue were analyzed (the rest of the sequencing results are shown in Figure S3C). The sequence between two guide RNAs is removed and shown as a reference

Cdh1 loci and up to 40% at the *Lmna* locus (Figure 3B,C). In the thymus, part of the EGFP-positive population moved to mCherry positive with a decrease in the EGFP signal (Figure 3D). Total indel frequencies at the *EGFP* locus in the mCherry-positive population reached greater than 80%, whereas that of the *Cdh1* and *Lmna*

loci were <20% (Figure 3C). These differences indicate that the responses to Dox substantially varied with the genomic locus, cell type and organ. Taken together, the RC platform enables efficient genome editing at multiple loci in somatic cells both in vitro and in vivo.

3.5 | Evaluation of impaired *Apc* function after genome editing in adult intestinal crypt cells

In CRISPR/Cas9-based genome editing, mutation patterns are heterogeneous and include in-frame shift mutations. Therefore, the efficiency of genome editing does not directly correlate with the efficiency of functional alterations of the targeted gene. It is also important to precisely assess leaky functional alterations in adult tissues, because we detected a subtle induction of genome editing in RC-MEF even in the absence of Dox. Previous studies showed that the Cre/loxP-mediated genetic deletion of *Apc* is sufficient for the inhibition of differentiation and the initiation of adenomatous crypts in the intestine,[20] indicating that a loss of *Apc* function causes immediate histological abnormalities. Considering that intestinal crypts are maintained by stem cells and that the replacement of most crypt cells occurs within a week, histological assessment of the adenomatous crypts can be used to precisely and quantitatively evaluate altered *Apc* function in adult intestinal cells.

To investigate the induction of functional alterations of the *Apc* gene in adult intestinal cells with the RC platform, we established EGFP-labeled RC-ES cells carrying a sgRNA targeting exon 16 of the *Apc* gene and generated chimeric mice (Figure 4A,B). These mice were histologically examined for the incidence of adenomatous crypts in EGFP-labeled crypts in the presence and absence of Dox. Notably, we observed no evidence of impaired differentiation or adenomatous crypt formation in the EGFP-positive intestinal crypts of Dox-untreated RC-mice (total of 331 EGFP-positive crypts from three mice, Figure 4C,D). In contrast, giving Dox for 7 days induced adenomatous crypts showing an accumulation of cytoplasmic/nuclear β-catenin protein at varying frequencies (Figure 4C,D). One of three Dox-treated RC-mice did not show any adenomatous crypt formation in the intestine despite the presence of local contribution of ES cell-derived cells (Figure 4D). Together, we confirmed that functional alterations can be induced in adult somatic cells with the RC platform. Moreover, our results suggest that leaky functional alterations are negligible in the intestinal crypts of RC-mice.

3.6 | Modeling Wilms' tumor with *Ctnnb1* exon 3 deletion and indels at *Wt1* gene

To test whether the RC platform is practical for modeling cancer with complex genomic abnormalities, we first tried to recapitulate a

previously reported Wilms' tumor model with the activating mutation at *Ctnnb1* in conjunction with the inactivating mutation at *Wt1*.[21] In the previous study, *Ctnnb1* exon 3 was deleted by the conventional Cre/loxP system, which led to accumulation of the dominant stable form of β-catenin protein.[22,23] In our strategy, we designed two sgRNAs that flank exon 3 of *Ctnnb1* instead of two *loxP* sites, and one sgRNA to target exon 2 of *Wt1* (Figure 5A,B). Giving Dox starting at embryonic day 14.5-18.5 (E14.5-18.5) resulted in the growth retardation phenotype in Dox-treated RC-mice (Figure 5C). We also observed the development of kidney tumors and dilatation of the intestinal tract (Figure 5C). Notably, histological analysis showed that the kidney tumors had typical features of Wilms' tumor, which include blastemal, stromal, and epithelial components (Figure 5D,E). Among the analyzed mice (50% to 70% coat color chimerism in both cohorts), all of three Dox-treated mice showed both kidney and intestinal lesions whereas none of five Dox-untreated mice showed any macroscopic phenotypes nor histological abnormalities. Immunohistochemical staining confirmed the aberrant accumulation of β-catenin in both kidney tumors and intestinal adenomatous lesions (Figure 5D and Figure S3A). Six2, which is expressed in embryonic nephron progenitor cells and Wilms' tumor cells, was expressed in kidney tumor cells (Figure 5F). cDNA cloning and Sanger sequencing showed efficient genomic deletion of *Ctnnb1* exon 3 and frequent indels at the *Wt1* locus in the kidney, small intestine and colon of the chimeric mice but not of the non-chimeric mice (Figure 5G,H, Figure S3B,C). These results indicate that the RC platform is useful for inducing both activating and inactivating mutations at multiple loci in vivo, suggesting an alternative complex cancer model to the conventional and labor-intensive Cre/loxP-based method.

3.7 | Modeling intestinal adenoma progression by large genomic deletion at *H19* imprinting control region and indels at *Apc* gene

To examine whether a larger genomic deletion could be induced in vivo, we next sought to model the progression of intestinal adenoma by inducing a genomic deletion at the *H19* ICR together with indels at the *Apc* gene.[24] CTCF (CCCTC-binding factor) proteins assemble at *H19* ICR, which generates a cis-acting, enhancer-blocking element for *Igf2* expression.[25] Consistently, genetic deletion of *H19* ICR causes increased *Igf2* expression. Given that increased *Igf2* expression is often involved in colon cancer development, we combined

FIGURE 6 Modeling intestinal adenoma progression by large genomic deletion at *H19* imprinting control region (ICR) and insertions and deletions (indels) at *Apc* gene. A, Strategy and design of single guide (sg)RNAs (red arrowheads) to induce *H19-ICR* genomic deletion and indels at *Apc* gene. Asterisk indicates indels. B,C, PCR to examine deletion of the *H19*-ICR locus (B) and TIDE analysis of indels at the *Apc* gene (C) in RC-embryonic stem (ES) cells after doxycycline (Dox) exposure for 72 h in vitro. Primers used (a and b, respectively) are indicated in (A). Non-targeted KH2 and V6.5 ES cells were used as control samples (B). Three distinct clones were assayed. D, Sanger sequencing of cDNA at the *H19*-ICR locus cloned from the PCR product of clone A in Figure 6B. The sequence between two sgRNAs is removed and shown as a reference. E, qRT-PCR analysis for *Igf2* in RC-ES cells. Relative expressions to β-*actin* are shown. Expression levels of the non-treated clones were set to 1. Data are shown as mean of technical triplicates. F, Histological analysis of RC-chimeric mice. The mice were treated with Dox starting at 4 weeks of age and analyzed at 5 weeks of age. Scale bars, 200 μm (upper panels) and 100 μm (lower panels). (G) Mitotic figures in adenomatous lesions. Total of 27 distinct lesions from three mice with sg*Apc*/*H19*-ICR and 45 lesions from five mice with sg*Apc* alone were analyzed. Coat color chimerism were 10%-70% in both cohorts. Data are shown as median with interquartile range. **$P < .01$ (Mann-Whitney *U* test)

(A)

(B)

RC-ES cells (sg*Apc/H19*)

(C)

(D)

RC-ES cells (sg*Apc/H19*)

(E)

(F) RC-mice (sg*Apc/H19*)

(G)
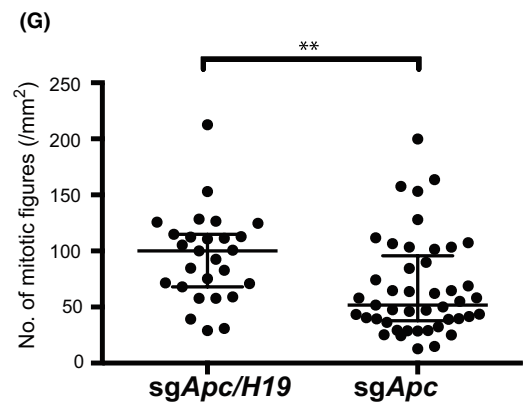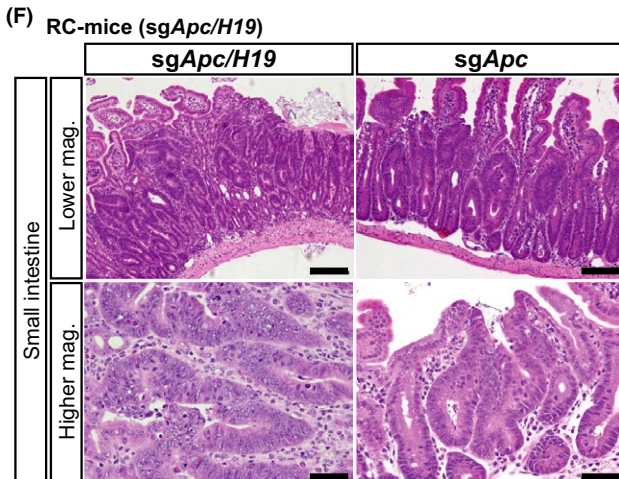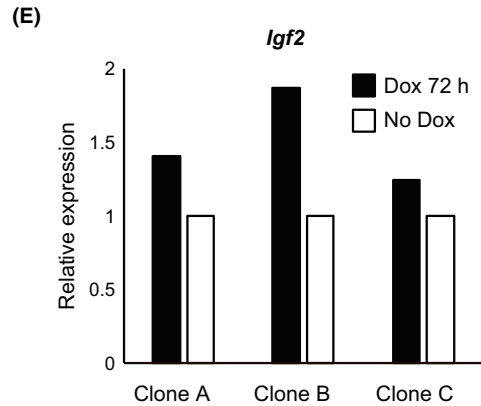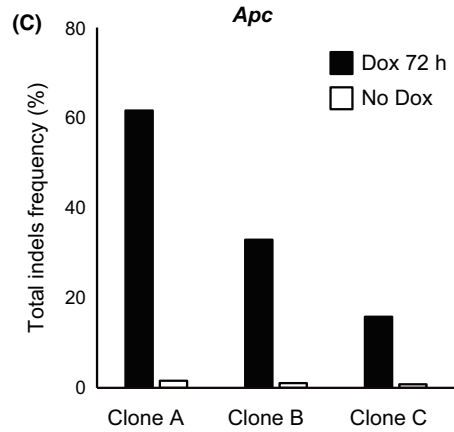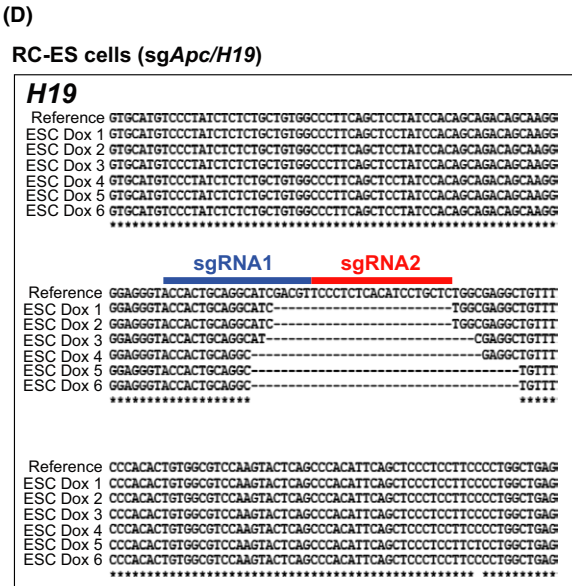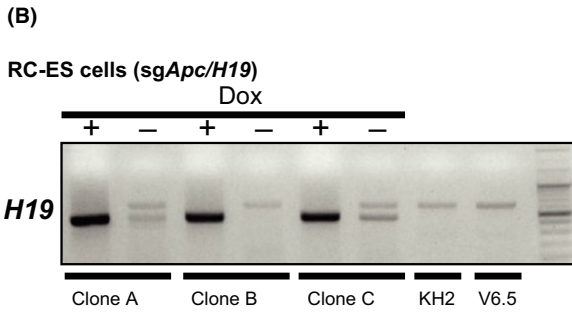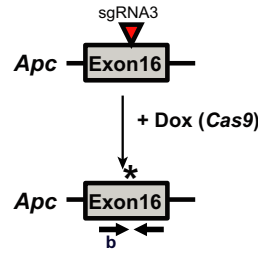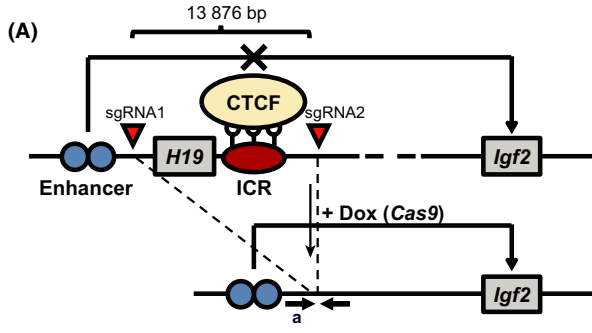
two previously reported sgRNAs to delete the *H19* ICR locus,[26] which spans more than 13 kb, in addition to one sgRNA to target exon 16 of *Apc* to model the progression of intestinal tumorigenesis (Figure 6A). After giving Dox in vitro, genomic deletions at *H19* ICR and indels at *Apc* were efficiently generated in RC-ES cells (Figure 6B,C). We found that the *H19* ICR locus was precisely removed between the two sgRNA-targeted sites (Figure 6D) and the concomitant upregulation of *Igf2* expression was detectable in Dox-treated RC-ES cells (Figure 6E). RC-mice showed adenomatous lesions in the intestine after 1 week of Dox treatment (Figure 6F). Importantly, we confirmed that Dox treatment successfully induced a large deletion at the *H19*-ICR locus in vivo (Figure S4A,B). Moreover, histological analysis showed that adenomatous lesions in RC-mice targeting both the *H19* ICR and *Apc* gene showed higher frequency of mitotic counts when compared with single mutant mice for the *Apc* gene (Figure 6F,G and Figure S4C). Taken together, complex mutations including a large genomic deletion are efficiently inducible in somatic cells in vivo with the RC platform.

4 | DISCUSSION

A Dox-inducible *Cas9*-based RC platform, which has *rtTA* at the *Rosa26* locus and *TRE-Cas9* allele together with multiple sgRNAs at the *Col1a1* locus, successfully achieved efficient genome editing at multiple loci for complex cancer modeling with much less labor than conventional methods. MultiSite Gateway technology allowed us to combine up to four sgRNAs simultaneously and, therefore, the entire vector construction could be finished within a week, providing a more flexible system than the previously reported platform.[8] Application of the Golden Gate cloning-based system[27] may be useful to further increase the number of targeting loci for genome editing.

It is noteworthy that the R platform, which contains all transgenic components in one construct at the *Rosa26* locus, showed significant frequency of leaky indels in the absence of Dox exposure, and showed little improvement in genome editing in response to Dox treatment. These findings suggested that the targeted loci for the Dox-inducible components were important in order to tightly control conditional genome editing with an inducible *Cas9* system. Positioning of *rtTA* and *TRE* in the inverse direction[28] or using an inducible sgRNA expression system[29] might be useful for rigorous control of genome editing with an inducible *Cas9* system.

Finally, we succeeded in modeling cancers with complex genetic abnormalities in an inducible method, including the induction of a large genomic deletion ranging over 13 kb. Efficiencies of the genomic deletion were high enough for mutated alleles to be dominant, indicating that our platform could substitute conventional recombinase-based methods such as Cre/loxP in some cases. Although it should be noted that the induced mutation patterns were heterogeneous and included in-frame shift mutations, recent reports suggested that the frequency of out-of-frame shift mutations could be increased by selecting a target site flanked by microhomology, resulting in efficient gene knockout.[30,31]

Recently, various genomic modifications with CRISPR/Cas9 technology have been reported, including genomic translocation,[32,33] inversion, chromosome elimination,[34,35] single point mutation and knock-in.[36] Combining these genome-editing technologies with the RC platform will further facilitate diverse cancer modeling and functional assays in vivo, which should deepen our understanding of the mechanisms that govern various biological phenomena in mammals in vivo.

CONFLICTS OF INTEREST

Authors declare no conflicts of interest for this article.

ORCID

Yasuhiro Yamada https://orcid.org/0000-0002-2463-1478

REFERENCES

1. Hsu PD, Lander ES, Zhang F. Development and applications of CRISPR-Cas9 for genome engineering. *Cell.* 2014;157(6):1262-1278.
2. Dow LE. Modeling disease in vivo with CRISPR/Cas9. *Trends Mol Med.* 2015;21(10):609-621.
3. Wang H, Yang H, Shivalila CS, et al. One-step generation of mice carrying mutations in multiple genes by CRISPR/Cas-mediated genome engineering. *Cell.* 2013;153(4):910-918.
4. Swiech L, Heidenreich M, Banerjee A, et al. In vivo interrogation of gene function in the mammalian brain using CRISPR-Cas9. *Nat Biotechnol.* 2015;33(1):102-106.
5. Maresch R, Mueller S, Veltkamp C, et al. Multiplexed pancreatic genome engineering and cancer induction by transfection-based CRISPR/Cas9 delivery in mice. *Nat Commun.* 2016;7:10770.
6. Platt RJ, Chen S, Zhou Y, et al. CRISPR-Cas9 knockin mice for genome editing and cancer modeling. *Cell.* 2014;159(2):440-455.
7. Wang K, Jin Q, Ruan D, et al. Cre-dependent Cas9-expressing pigs enable efficient in vivo genome editing. *Genome Res.* 2017;27(12):2061-2071.
8. Dow LE, Fisher J, O'Rourke KP, et al. Inducible in vivo genome editing with CRISPR/Cas9. *Nat Biotechnol.* 2015;33(4):390-394.
9. Cheo DL, Titus SA, Byrd DR, Hartley JL, Temple GF, Brasch MA. Concerted assembly and cloning of multiple DNA segments using in vitro site-specific recombination: functional analysis of multi-segment expression clones. *Genome Res.* 2004;14(10B):2111-2120.
10. Beard C, Hochedlinger K, Plath K, Wutz A, Jaenisch R. Efficient method to generate single-copy transgenic mice by site-specific integration in embryonic stem cells. *Genesis.* 2006;44(1):23-28.
11. Hochedlinger K, Yamada Y, Beard C, Jaenisch R. Ectopic expression of Oct-4 blocks progenitor-cell differentiation and causes dysplasia in epithelial tissues. *Cell.* 2005;121(3):465-477.

12. Ohnishi K, Semi K, Yamamoto T, et al. Premature termination of reprogramming in vivo leads to cancer development through altered epigenetic regulation. *Cell*. 2014;156(4):663-677.

13. Komura S, Semi K, Itakura F, et al. An EWS-FLI1-induced osteosarcoma model unveiled a crucial role of impaired osteogenic differentiation on osteosarcoma development. *Stem Cell Reports*. 2016;6(4):592-606.

14. Albers J, Danzer C, Rechsteiner M, et al. A versatile modular vector system for rapid combinatorial mammalian genetics. *J Clin Invest*. 2015;125(4):1603-1619.

15. Yagi M, Kishigami S, Tanaka A, et al. Derivation of ground-state female ES cells maintaining gamete-derived DNA methylation. *Nature*. 2017;548(7666):224-227.

16. Shimizu T, Ueda J, Ho JC, et al. Dual inhibition of Src and GSK3 maintains mouse embryonic stem cells, whose differentiation is mechanically regulated by Src signaling. *Stem Cells*. 2012;30(7):1394-1404.

17. Kim SI, Oceguera-Yanez F, Sakurai C, Nakagawa M, Yamanaka S, Woltjen K. Inducible transgene expression in human iPS cells using versatile all-in-one piggyBac transposons. *Methods Mol Biol*. 2016;1357:111-131.

18. Brinkman EK, Chen T, Amendola M, van Steensel B. Easy quantitative assessment of genome editing by sequence trace decomposition. *Nucleic Acids Res*. 2014;42(22):e168.

19. Ran FA, Hsu PD, Wright J, Agarwala V, Scott DA, Zhang F. Genome engineering using the CRISPR-Cas9 system. *Nat Protoc*. 2013;8(11):2281-2308.

20. Sansom OJ, Reed KR, Hayes AJ, et al. Loss of Apc in vivo immediately perturbs Wnt signaling, differentiation, and migration. *Genes Dev*. 2004;18(12):1385-1390.

21. Huang L, Mokkapati S, Hu Q, Ruteshouser EC, Hicks MJ, Huff V. Nephron progenitor but not stromal progenitor cells give rise to Wilms tumors in mouse models with β-catenin activation or Wt1 ablation and Igf2 upregulation. *Neoplasia*. 2016;18(2):71-81.

22. Harada N, Miyoshi H, Murai N, et al. Lack of tumorigenesis in the mouse liver after adenovirus-mediated expression of a dominant stable mutant of beta-catenin. *Cancer Res*. 2002;62(7):1971-1977.

23. Harada N, Tamai Y, Ishikawa T, et al. Intestinal polyposis in mice with a dominant stable mutation of the beta-catenin gene. *EMBO J*. 1999;18(21):5931-5942.

24. Sakatani T, Kaneda A, Iacobuzio-Donahue CA, et al. Loss of imprinting of Igf2 alters intestinal maturation and tumorigenesis in mice. *Science*. 2005;307(5717):1976-1978.

25. Hark AT, Schoenherr CJ, Katz DJ, Ingram RS, Levorse JM, Tilghman SM. CTCF mediates methylation-sensitive enhancer-blocking activity at the H19/Igf2 locus. *Nature*. 2000;405(6785):486-489.

26. Zhang M, Liu Y, Liu G, et al. Rapidly generating knockout mice from H19-Igf2 engineered androgenetic haploid embryonic stem cells. *Cell Discov*. 2015;1:15031.

27. Sakuma T, Nishikawa A, Kume S, Chayama K, Yamamoto T. Multiplex genome engineering in human cells using all-in-one CRISPR/Cas9 vector system. *Sci Rep*. 2014;4:5400.

28. Mandegar MA, Huebsch N, Frolov EB, et al. CRISPR interference efficiently induces specific and reversible gene silencing in human iPSCs. *Cell Stem Cell*. 2016;18(4):541-553.

29. Aubrey BJ, Kelly GL, Kueh AJ, et al. An inducible lentiviral guide RNA platform enables the identification of tumor-essential genes and tumor-promoting mutations in vivo. *Cell Rep*. 2015;10(8):1422-1432.

30. Bae S, Kweon J, Kim HS, Kim JS. Microhomology-based choice of Cas9 nuclease target sites. *Nat Methods*. 2014;11(7):705-706.

31. Kim SI, Matsumoto T, Kagawa H, et al. Microhomology-assisted scarless genome editing in human iPSCs. *Nat Commun*. 2018;9(1):939.

32. Maddalo D, Manchado E, Concepcion CP, et al. In vivo engineering of oncogenic chromosomal rearrangements with the CRISPR/Cas9 system. *Nature*. 2014;516(7531):423-427.

33. Blasco RB, Karaca E, Ambrogio C, et al. Simple and rapid in vivo generation of chromosomal rearrangements using CRISPR/Cas9 technology. *Cell Rep*. 2014;9(4):1219-1227.

34. Adikusuma F, Williams N, Grutzner F, Hughes J, Thomas P. Targeted deletion of an entire chromosome using CRISPR/Cas9. *Mol Ther*. 2017;25(8):1736-1738.

35. Zuo E, Huo X, Yao X, et al. CRISPR/Cas9-mediated targeted chromosome elimination. *Genome Biol*. 2017;18(1):224.

36. Paquet D, Kwart D, Chen A, et al. Efficient introduction of specific homozygous and heterozygous mutations using CRISPR/Cas9. *Nature*. 2016;533(7601):125-129.

SUPPORTING INFORMATION

Additional supporting information may be found online in the Supporting Information section at the end of the article.